Optical Materials 37 (2014) 257–261

Contents lists available at ScienceDirect

Optical Materials

journal homepage: www.elsevier.com/locate/optmat

Spectroscopic properties of $HoAl_3(BO_3)_4$ single crystal

D.A. Ikonnikov [a], A.V. Malakhovskii [b], A.L. Sukhachev [b], V.L. Temerov [b], A.S. Krylov [b], A.F. Bovina [b], A.S. Aleksandrovsky [b,*]

[a] Siberian Federal University, Krasnoyarsk, Russia
[b] L.V. Kirensky Institute of Physics, Siberian Branch, Russian Academy of Sciences, 660036 Krasnoyarsk, Russia

ARTICLE INFO

Article history:
Received 10 March 2014
Received in revised form 29 May 2014
Accepted 30 May 2014
Available online 27 June 2014

Keywords:
Absorption
Luminescence
Holmium
Huntite
Judd–Ofelt

ABSTRACT

The Judd–Ofelt theory has been applied to analyze absorption spectra of Ho^{3+} ion in $HoAl_3(BO_3)_4$ measured in spectral range 300–700 nm at room temperature. The Judd–Ofelt spectroscopic parameters have been determined as: $\Omega_2 = 18.87 \times 10^{-20}$ cm^2, $\Omega_4 = 17.04 \times 10^{-20}$ cm^2, $\Omega_6 = 9.21 \times 10^{-20}$ cm^2. These parameters have been used to calculate radiative lifetimes and branching ratios of the luminescence manifolds. Three luminescent bands were found in the spectral range 450–700 nm ascribed to transitions from the $^5F_5$, ($^5F_4$, $^5S_2$) and $^3K_8$ states to the ground state $^5I_8$. Experimental intensities of these luminescence transitions were compared with those calculated by using Judd–Ofelt theory and the system of kinetic equations for populations of starting luminescing states. Probabilities of radiativeless transitions were evaluated from this comparison.

1. Introduction

Borates $RAl_3(BO_3)_4$ (R–Y or rare earth metal) have huntite-like structure. These crystals have excellent chemical and physical properties. They also have rather high nonlinear susceptibility of the second order and may be used as polyfunctional materials for photonic devices creation. They are of interest for the luminescence study, since some of them have relatively small luminescence quenching when rare-earth element concentration is increased.

Ho^{3+} is well-known active ion in solid state lasers with the emissions in the infrared and visible spectral ranges. Optical properties of Ho^{3+} ion were studied in many materials (e. g. [1–8]). The visible and near-infrared luminescence in $Ho:YAl_3(BO_3)_4$ crystal was investigated by Koporulina et al. [9]. But to our knowledge, spectroscopic properties of the stoichiometric $HoAl_3(BO_3)_4$ crystal were not studied in detail, and Judd–Ofelt analysis was not done for this crystal. Additional interest to $HoAl_3(BO_3)_4$ may arise from the point of view of multifunctionality, since giant magnetoelectric effect was found for this crystal [10]. Another possible application of Ho ions in huntite structure is the quantum manipulation medium as discussed in [11], where detailed study of hyperfine and crystal field splitting is presented for $Ho:YAl_3(BO_3)_4$ crystal. Upconversion luminescence was studied in $Ho,Yb:YAl_3(BO_3)_4$ [12], and two weak luminescent lines in the visible were detected.

The aim of the present study is the measurement of the absorption spectra for σ- and π-polarizations, detailed Judd–Ofelt analysis for the $HoAl_3(BO_3)_4$ crystal, and comparison of experimental and theoretical intensities of luminescent transitions. For the latter purpose, system of kinetic equations was derived with account for radiativeless transitions involved in the excitation channels.

2. Experimental

$HoAl_3(BO_3)_4$ single crystals were grown from lithium molybdate and bismuth trimolybdate based fluxes [13]. The fluxes with a weight of 1 kg were prepared at $T = 1000$ °C in cylindrical platinum crucible ($D = 100$ mm, $H = 90$ mm) by melting of reagent grade oxides [Bi_2O_3, MoO_3, Li_2CO_3, B_2O_3, Ho_2O_3, Al_2O_3]. The crucible was placed in a crystallization furnace, where the temperature was reduced from the crucible bottom with a vertical gradient of 1–2 °C/cm. Flux was homogenized at $T = 1000$ °C for 24 h. To keep homogeneity, the flux was stirred.

First, in the regime of spontaneous nucleation at $T = T_{sat}-(15-20)$ °C grown crystals of ~1 mm. In this case the crystal holder with small grown crystals pulled out without the temperature changing in the furnace. These crystals were then used as seeds.

After that 10–12 visual quality seeds were attached to the Pt ring-shaped holder. The holder was immersed in the flux at $T = T_{sat} + 7$ °C and the reversible rotation with a period of 1 min at $\omega = 30$ rpm was turned on. After 15 min, the temperature was lowered to $T = T_{sat}-7$ °C. Then, the temperature was decreased at

* Corresponding author. Tel.: +7 391 2494613.
E-mail address: aleksandrovsky@kirensky.ru (A.S. Aleksandrovsky).

http://dx.doi.org/10.1016/j.optmat.2014.05.036
0925-3467/

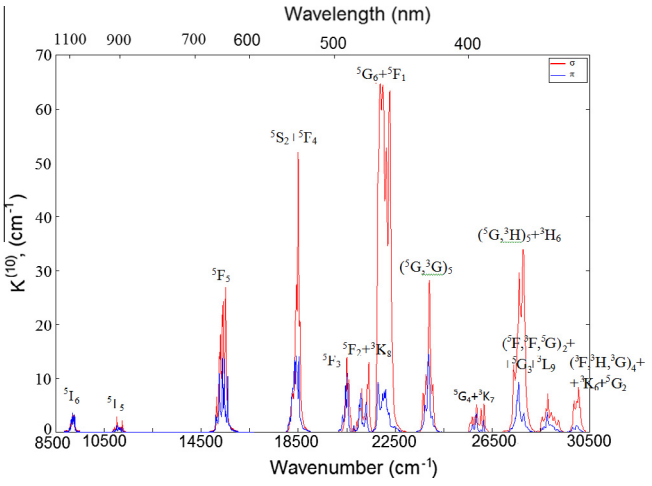

Fig. 1. Polarized absorption spectra of $HoAl_3(BO_3)_4$ taken at room temperature.

an increasing rate within 1–2 °C/day, so that the crystal growth rate does not exceed 0.5 mm per day. After the 9–10 days growth, crystals of about 5–7 mm in size were obtained. They were of excellent optical quality with no inclusions and possessed growth habit perfectly corresponding to that known for huntite.

Crystal structure of $HoAl_3(BO_3)_4$ crystal was determined with the help of Bruker D8 Advance X-ray diffractometer to belong to the space group $R32$ of trigonal symmetry class. Unit cell parameters are found to be $a = 9.3097(5)$ Å, $c = 7.1887(4)$ Å. Absorption spectra were obtained with the light propagating normally to the C_3 axis of the crystal for the light electric vector $\vec{E}$ ether parallel (π spectrum) or perpendicular (σ spectrum) to the C_3 axis. The thickness of the sample was 0.24 mm. Absorption spectra of Ho^{3+} ion in $HoAl_3(BO_3)_4$ were measured with a double-beam spectrometer in the spectral range 300–700 nm at room temperature. The luminescence spectra were measured within spectral range 450–700 nm using Horiba Jobin–Yvon T64000 spectrometer with excitation at 457.9 nm through $^5G_6$ energy level of holmium ion. Exciting radiation propagated along C_3 axis, and unpolarized luminescence was collected in backward direction.

3. Theoretical

Intensities of absorption bands in π- and σ-polarizations were found as integrals $I_{IF} = \int \frac{K^{(10)}(E)}{C} dE$ over the bands, where $K^{(10)} = \frac{1}{d}\lg\frac{I_0}{I}$, I and I_0 are intensities of probe and reference beams, C is the molar concentration in mol/l and E is the quantum energy in cm^{-1}. The transition intensities were averaged over the polarizations according to common relation for uniaxial anisotropic crystals: $I_{IF} = (2I^{\sigma}_{IF} + I^{\pi}_{IF})/3$. The oscillator strengths of transitions $I \to F$ between J multiplets were calculated by the formula:

$$f_{IF} = 4.318 \times 10^{-9} \frac{3n}{(n)^2 + 2} I_{If}, \quad (1)$$

Refractive index n of alumoborates slightly depends on rare earth ion. There are no experimental data for the crystal under study up to date, and we used the approximation earlier used for Judd–Ofelt analysis of $ErAl_3(BO_3)_4$ [14] that refractive index of $HoAl_3(BO_3)_4$ over the entire spectral range is equal to 1.75 with accuracy of ±3%. This error results in ±0.7% error of oscillator strengths calculation according to (1).

The transition strength is defined as:

$$s_{IF} = \frac{3hg_I}{8\pi^2 mck_{IF}} f_{IF}, \quad (2)$$

where g_I is the degree of degeneracy of the initial state and k_{IF} is the average wave number of the absorption band.

In the framework of the J–O theory [15–17], the strength of an f–f transition is described by the relationship

$$s_{IF} = \sum_{\lambda} \Omega_{\lambda} I^2_{\lambda}(I, F), \quad (3)$$

Error of the theoretical description of the transition strengths is defined by equation:

$$\Delta = \left[\frac{q \sum \Delta s^2}{(q-p)\sum s^2}\right]^{1/2}. \quad (4)$$

where

s are measured transition strengths;
Δs are differences between the measured and calculated transition strengths;
q is number of transitions;
p is number of the determined parameters Ω, in our case being equal to 3.

The distribution of the luminescence intensities between specific emission channels is characterized by the multiplet luminescence branching ratio

$$\beta_{IF} = A_{IF} / \sum_{F} A_{IF} = A_{IF}\tau_I, \quad (5)$$

where τ_I is the excited state life time; $A_{IF} = \frac{64\pi^4 e^2 k^3_{IF} n}{3hg_I} s_{IF}$ are spontaneous transition probabilities; g_I are degeneracies of starting multiplets; n is the refraction index.

For comparison of relative intensities of different luminescence bands, theoretical integral intensities of luminescence at I–F transitions were calculated:

Table 1
Optical characteristics of Ho^{3+} ion in $HoAl_3(BO_3)_4$.

Transition $^5I_8 \to$	k_{IF} ($см^{-1}$)	I_{IF} ($cm^{-2}mol^{-1}l$)		f_{IF} (10^{-7})	s_{IF} (10^{-20} cm^2)	
		σ	π		Measured	Calculated
$^5I_6$	8900	546.572	644.625	26.06	2.07	7.18
$^5I_5$	11150	226.582	430.922	15.45	0.94	1.03
$^5F_5$	15380	4281	5873	199.9	12.00	12.48
$^5S_2 + {}^5F_4$	18450	2335	8912	313.8	15.71	12.68
$^5F_3$	20490	1618	2109	82.86	3.74	3.19
$^5F_2 + {}^3K_8$	21190	1458	2818	100.7	4.40	4.18
$^5G_6 + {}^5F_1$	22080	3635	35010	1046	43.76	44.31
$(^5G,{}^3G)_5$	23810	2769	12510	203	7.88	9.10
$^5G_4 + {}^3K_7$	25970	611.796	5765	57.86	2.06	1.37
$(^5G,{}^3H)_5 + {}^3H_6$	27620	2224	1732	386.7	12.93	8.93
$(^5F,{}^3F,{}^5G)_2 + {}^5G_3 + {}^3L_9$	28740	825.76	2392	79.63	2.56	2.01
$(^3F,{}^3H,{}^3G)_4 + {}^3K_6 + {}^5G_2$	29940	328.511	2126	65.02	2.01	2.28

Table 2
Judd–Ofelt parameters Ω_i for Ho^{3+} in different hosts.

Compound	Ω_2, 10^{-20} cm^2	Ω_4, 10^{-20} cm^2	Ω_6, 10^{-20} cm^2
$HoAl_3(BO_3)_4$	18.87	17.04	9.21
Ho:PBG [6]	6.81	2.31	0.67
Ho:$LiTaO_3$ [7]	12.6	6.1	4.3
Ho:YAG [19]	0.101	2.086	1.724
HoP_5O_{14} [20]		1.4	1.46
Ho:InF_3–ZnF_2–SrF_2 [21]	1.37	2.35	2.22
Ho:Li_2O–K_2O–BaO–Bi_2O_3–TeO_2 [22]	4.37	1.91	1.45
Ho:PbO–Al_2O_3–B_2O_3 [23]	5.83	17.15	26.5
Ho:LaF_5 [24]	1.16	1.38	0.88
Ho:$YAlO_3$ [25]	1.82	2.38	1.53
Ho:KGW [26]	10.14	3.09	1.99

Table 3
The branching ratios of the *f*–*f* transitions of holmium luminescence manifolds in $HoAl_3(BO_3)_4$.

Transition	k_{IF} (cm^{-1})	s_{IF} (10^{-20} cm^2)	β_{if}
$^5G_6$–$^3K_8$	850	2.359	3.342×10^{-6}
$^5G_6$–$^5F_2$	1150	1.162	5.008×10^{-6}
$^5G_6$–$^5F_3$	1600	1.789	2.355×10^{-5}
$^5G_6$–$^5F_4$,$^5S_2$	3700	10.16	1.755×10^{-3}
$^5G_6$–$^5F_5$	6700	28.59	0.019
$^5G_6$–$^5I_4$	8950	0.019	5.029×10^{-5}
$^5G_6$–$^5I_5$	11,000	0.664	2.812×10^{-3}
$^5G_6$–$^5I_6$	13,550	1.649	0.014
$^5G_6$–$^5I_7$	17,050	6.027	0.066
$^5G_6$–$^5I_8$	22,150	32.182	0.897
$^3K_8$–$^5F_2$	250	4.459×10^{-6}	2.754×10^{-9}
$^3K_8$–$^5F_3$	750	0.055	9.22×10^{-7}
$^3K_8$–$^5F_4$,$^5S_2$	2850	0.049	1.241×10^{-4}
$^3K_8$–$^5F_5$	5850	0.319	4.809×10^{-3}
$^3K_8$–$^5I_4$	8100	0.035	1.784×10^{-3}
$^3K_8$–$^5I_5$	10,150	0.039	1.784×10^{-3}
$^3K_8$–$^5I_6$	12,700	0.28	0.024
$^3K_8$–$^5I_7$	16,200	0.431	0.079
$^3K_8$–$^5I_8$	21,250	2.069	0.888
$^5F_4$,$^5S_2$–$^5F_5$	3000	5.112	1.373×10^{-3}
$^5F_4$,$^5S_2$–$^5I_4$	5250	5.104	7.743×10^{-3}
$^5F_4$,$^5S_2$–$^5I_5$	7300	5.886	0.027
$^5F_4$,$^5S_2$–$^5I_6$	9850	4.447	0.068
$^5F_4$,$^5S_2$–$^5I_7$	13,350	5.035	0.163
$^5F_4$,$^5S_2$–$^5I_8$	18,450	9.659	0.733
$^5F_5$–$^5I_4$	2250	0.038	3.646×10^{-4}
$^5F_5$–$^5I_5$	4300	1.775	4.864×10^{-3}
$^5F_5$–$^5I_6$	6850	5.355	0.031
$^5F_5$–$^5I_7$	10,350	6.089	0.163
$^5F_5$–$^5I_8$	15,400	7.423	0.8

$$I_{IF} \approx N_I \cdot A_{IF}, \tag{6}$$

where N_I is the population of I-th energy level; A_{IF} were obtained via Judd–Ofelt theory. To calculate populations of multiplets involved into luminescence we initially used kinetic equations system that takes into account only radiative transitions:

$$\begin{cases} \frac{dN_{^5G_6}}{dt} = W_p N_{^5I_8} - \frac{N_{^5G_6}}{\tau_{^5G_6}} \\ \frac{dN_{^3K_8}}{dt} = \frac{N_{^5G_6}}{\tau_{^5G_6-{}^3K_8}} - \frac{N_{^3K_8}}{\tau_{^3K_8}} \\ \frac{dN_{^5F_4,{}^5S_2}}{dt} = \frac{N_{^5G_6}}{\tau_{^5G_6-{}^5F_4,{}^5S_2}} + \frac{N_{^3K_8}}{\tau_{^3K_8-{}^5F_4,{}^5S_2}} - \frac{N_{^5F_4,{}^5S_2}}{\tau_{^5F_4,{}^5S_2}} \\ \frac{dN_{^5F_5}}{dt} = \frac{N_{^5G_6}}{\tau_{^5G_6-{}^5F_5}} + \frac{N_{^3K_8}}{\tau_{^3K_8-{}^5F_5}} + \frac{N_{^5F_4,{}^5S_2}}{\tau_{^5F_4,{}^5S_2-{}^5F_5}} - \frac{N_{^5F_5}}{\tau_{^5F_5}} \\ \frac{dN_{^5I_8}}{dt} = \frac{N_{^5G_6}}{\tau_{^3G_6-{}^5I_8}} + \frac{N_{^3K_8}}{\tau_{^3K_8-{}^5I_8}} + \frac{N_{^5F_4,{}^5S_2}}{\tau_{^5F_4,{}^5S_2-{}^5I_8}} + \frac{N_{^5F_5}}{\tau_{^5F_5-{}^5I_8}} - W_p N_{^5I_8} \end{cases}, \tag{7}$$

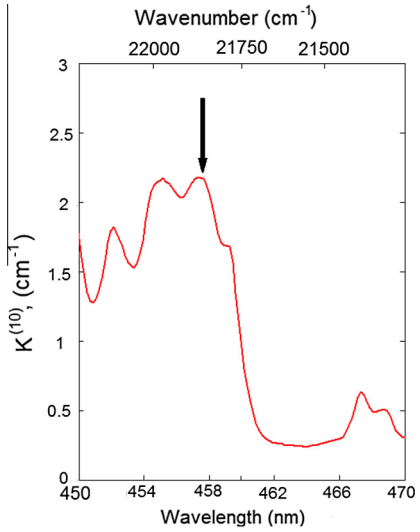

Fig. 2. Room temperature absorption spectrum of $HoAl_3(BO_3)_4$ in the vicinity of excitation wavelength (457.9 nm).

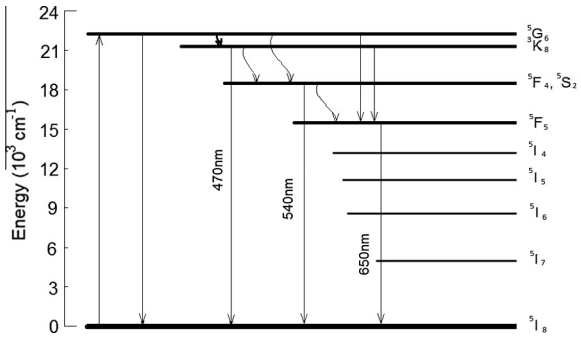

Fig. 3. The scheme of Ho^{3+} transitions involved in the processes of excitation and luminescence.

where $\tau_{1-F} = \frac{1}{A_{IF}}$; τ_I is radiative lifetime of I-th multiplet. W_p is probability of stimulated transition from ground state $^5I_8$ to excitation state $^5G_6$.

As will be seen from Section 4, Eq. (7) does not allow to predict experimental ratio between intensities of observed luminescence bands. To obtain better agreement, we used generalized kinetic equations system involving radiativeless relaxation in the excitation channels:

$$\begin{cases} \frac{dN_{^5G_6}}{dt} = W_p N_{^5I_8} - \frac{N_{^5G_6}}{\tau_{^5G_6}} - \frac{N_{^5G_6}}{\tau^{rl}_{^5G_6-{}^3K_8}} - \frac{N_{^5G_6}}{\tau^{rl}_{^5G_6-{}^5F_4,{}^5S_2}} \\ \frac{dN_{^3K_8}}{dt} = \frac{N_{^5G_6}}{\tau_{^5G_6-{}^3K_8}} - \frac{N_{^3K_8}}{\tau_{^3K_8}} + \frac{N_{^5G_6}}{\tau^{rl}_{^5G_6-{}^3K_8}} - \frac{N_{^3K_8}}{\tau^{rl}_{^3K_8-{}^5F_4,{}^5S_2}} \\ \frac{dN_{^5F_4,{}^5S_2}}{dt} = \frac{N_{^5G_6}}{\tau_{^5G_6-{}^5F_4,{}^5S_2}} + \frac{N_{^3K_8}}{\tau_{^3K_8-{}^5F_4,{}^5S_2}} - \frac{N_{^5F_4,{}^5S_2}}{\tau_{^5F_4,{}^5S_2}} + \frac{N_{^5G_6}}{\tau^{rl}_{^5G_6-{}^5F_4,{}^5S_2}} + \frac{N_{^3K_8}}{\tau^{rl}_{^3K_8-{}^5F_4,{}^5S_2}} - \frac{N_{^5F_4,{}^5S_2}}{\tau^{rl}_{^5F_4,{}^5S_2-{}^5F_5}}, \\ \frac{dN_{^5F_5}}{dt} = \frac{N_{^5G_6}}{\tau_{^5G_6-{}^5F_5}} + \frac{N_{^3K_8}}{\tau_{^3K_8-{}^5F_5}} + \frac{N_{^5F_4,{}^5S_2}}{\tau_{^5F_4,{}^5S_2-{}^5F_5}} - \frac{N_{^5F_5}}{\tau_{^5F_5}} + \frac{N_{^5F_4,{}^5S_2}}{\tau^{rl}_{^5F_4,{}^5S_2-{}^5F_5}} \\ \frac{dN_{^5I_8}}{dt} = \frac{N_{^5G_6}}{\tau_{^5G_6-{}^5I_8}} + \frac{N_{^3K_8}}{\tau_{^3K_8-{}^5I_8}} + \frac{N_{^5F_4,{}^5S_2}}{\tau_{^5F_4,{}^5S_2-{}^5I_8}} + \frac{N_{^5F_5}}{\tau_{^5F_5-{}^5I_8}} - W_p N_{^5I_8} \end{cases} \tag{8}$$

where $\tau^{rl}_{I-F} = \frac{1}{p_{IF}}$; p_{IF} are radiativeless relaxation probabilities.

4. Results and discussion

Absorption spectra of $HoAl_3(BO_3)_4$ crystal for σ- and π-polarizations at room temperature are shown in Fig. 1. Experimental integral intensities of absorption *f*–*f* transitions, I_{IF}, the oscillator

strengths (Eq. (1)) and transition strengths (Eq. (2)) were calculated from these spectra. Parameters Ω_i were determined via Judd–Ofelt analysis, and theoretical strengths of the studied transitions obtained from from Judd–Ofelt theory were found by Eq. (3) and compared with experimental ones. In our case residual discrepancy of the method Δ = 16.39, that is acceptable for Judd–Ofelt theory. Parameters Γ_λ^2 are taken from [18]. Results of analysis are given in Table 1. Parameters Ω determined for $HoAl_3(BO_3)_4$ are presented in Table 2 in comparison with those for Ho^{3+} ion in several other hosts[6–7,19–26].

One can see that parameter Ω_2 for $HoAl_3(BO_3)_4$ is the largest among all hosts listed in Table 2. But its contribution in transition strengths is usually insignificant, since coefficients Γ_2^2 [18] are extremely small for most transitions (often they are exactly zero). For laser transition at 2.1 μm from $^5I_7$ to $^5I_8$ it is equal 0.0249. Contribution from Ω_2 is significant only for two transitions covered by our measurement, namely, transition from excitation state $^5G_6$ to one of starting luminescent multiplets $^5F_5$ with the most intense luminescence ($\Gamma_2^2 = 1.1528$) and transition between $^5G_6$ and ground state $^5I_8$ ($\Gamma_2^2 = 1.5211$).

Calculated values of the transition strengths, the spontaneous emission probabilities, the branching ratios of the transitions and lifetimes of the states are presented in Table 3.

For luminescent studies, $HoAl_3(BO_3)_4$ crystal was excited at 457.9 nm i.e. through $^5G_6$ energy level (Fig. 2). Position of exciting radiation wavelength is indicated by arrow. Energy level scheme for "excitation–luminescence" transitions is shown on Fig. 3.

In difference with previous study of Ho ion luminescence in huntite host, where only one luminescent band was found in the visible [9], we observed three luminescent bands in the spectral

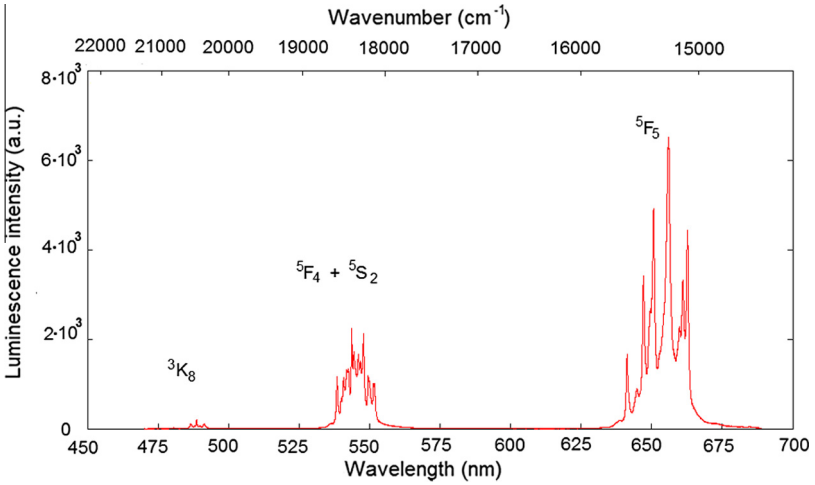

Fig. 4. Room temperature unpolarized luminescence spectrum of $HoAl_3(BO_3)_4$. Excitation wavelength 457.9 nm.

Table 4
Comparison of theoretical and experimental luminescence intensities.

Transition $\rightarrow {}^5I_8$	Integral intensity			Quadratic deviation, δ
	Calculated		Experimental	
	Without radiativeless transitions	With radiativeless transitions		
$^3K_8$	0.0002	0.01262	0.01262	5.04×10^{-6}
$^5F_4, {}^5S_2$	0.0791	0.30981	0.30987	
$^5F_5$	0.9207	0.67756	0.67751	

Table 5
Comparison of radiativeless transitions probabilities with radiative transitions probabilities and lifetime of initial levels.

Transition	Energy gap ΔE, cm^{-1}	τ_{IF}, s	τ_{IF}^{rl}, s	τ_I, s	Population of I-th level
$^5G_6\rightarrow$				5.72×10^{-6}	$W_p \times 10^{-8}$
$^3K_8$	850	1.71	$\sim 10^{-8}$		
$^5F_4, {}^5S_2$	3700	3.256×10^{-3}	$\sim 10^{-5}$		
$^5F_5$	6700	3.057×10^{-4}	$\gg\tau_{if}$		
$^5I_8$	22150	6.374×10^{-6}	$\gg\tau_{if}$		
$^3K_8 \rightarrow$				9.91×10^{-5}	W_p 1.1×10^{-6}
$^5F_4, {}^5S_2$	2850	0.798	1.111×10^{-6}		
$^5F_5$	5850	0.021	$\gg\tau_{if}$		
$^5I_8$	21250	1.116×10^{-4}	$\gg\tau_{if}$		
$^5F_4, {}^5S_2\rightarrow$				2.38×10^{-5}	W_p·7.8×10^{-6}
$^5F_5$	3000	0.017	1.188×10^{-5}		
$^5I_8$	18450	3.245×10^{-5}	$\gg\tau_{if}$		
$^5F_5\rightarrow$				3.68×10^{-8}	$W_p \times 2.43 \cdot 10^{-8}$
$^5I_8$	15400	4.602×10^{-8}	$\gg\tau_{if}$		

range 450–700 nm. The most intense of them is transition from $^5F_5$ to ground state $^5I_8$. The transition from two multiplets with the same energy $^5F_4$ и $^5S_2$ shows intermediate intensity, and the weakest transition is that from $^3K_8$. This luminescence pattern differs the crystal under study from a number of holmium-containing fluorides (see, e.g. [27]), where the luminescence from $^5S_2$ dominates (see Fig. 4).

Initially, we used Eq. (7) for calculation of luminescent multiplets' populations and then inserted those populations in Eq. (6) to determine theoretical integral intensities of luminescent transitions. The results obtained with Eq. (7) are presented in the second column of Table 4 in comparison with experimental ones (forth column).

As one can see from the second column of Table 4, the luminescence at $^5F_5$–$^5I_8$ transition is expected to be absolutely dominating, and two other transitions must show 20–2000 times smaller luminescence intensities. Experimental intensity at $^5F_4$,$^5S_2$–$^5I_8$ transition is only two times smaller. To obtain better agreement, let us introduce probabilities of radiativeless transitions as phenomenological parameters (Eq. (8)) to be determined from fitting with experiment. Results of this fitting are listed in the third column of Table 4.

In this Table,

$$\delta = \sqrt{\frac{1}{n}\sum_{i=1}^{n}(\chi_i - \bar{\chi})^2} \tag{9}$$

where $x = |I_{exp} - I_{culc}|$, n is the number of luminescent bands, I_{exp} is the experimental luminescent intensity, and I_{culc} is the intensity calculated with account for radiativeless transitions. δ here characterizes not accuracy of J–O method, but accuracy of phenomenological parameters definition. The phenomenological parameters of radiativeless transitions probabilities determined by this fitting are presented in Table 5. They are in reasonable agreement with radiativeless transitions theory [28–30]. W_p in the Table 5 is the pumping rate of $^5G_6$ state, that is, probability of excitation of holmium ion to $^5G_6$ from the ground state by the radiation at 457.9 nm. As one can see from Table 5, the maximum population is on $^5F_4$,$^5S_2$ states, and population of most intensely luminescing $^5F_5$ state is mainly due to radiativeless transition from $^5F_4$,$^5S_2$. However, probability of luminescence from $^5F_4$,$^5S_2$ is much smaller than that from $^5F_5$, that explains observed ratio of the luminescence intensities.

5. Conclusions

Absorption spectra for holmium ion in holmium alumoborate lattice for σ- and π-polarizations are measured and analyzed, and Judd–Ofelt parameters are found to be $\Omega_2 = 18.87 \times 10^{-20}$ cm^2, $\Omega_4 = 17.04 \times 10^{-20}$ cm^2, $\Omega_6 = 9.21 \times 10^{-20}$ cm^2. Three luminescent bands were found in the spectral range 450–700 nm ascribed to transitions from $^5F_5$, ($^5F_4$,$^5S_2$) and $^3K_8$ states to the ground state $^5I_8$. Experimental intensities of the luminescent lines strongly disagree with Judd–Ofelt predictions if only radiative transitions are involved, while taking radiativeless transitions into consideration allows to obtain good agreement. Probabilities of radiativeless transitions were evaluated from the system of kinetic equations for populations of starting luminescing states.

Acknowledgement

The work was supported by Grant of the Ministry of Education and Science of the Russian Federation for Siberian Federal University, the Russian Foundation for Basic Research Grants 12-02-00026, 14-02-00219 and 13-02-00825, by the Russian President Grant SS-2886.2014.2, and by SB RAS Project No. 43.

References

[1] Ch. Srinivasa Rao, K. Upendra Kumar, P. Babu, C.K. Jayasankar, Opt. Mater. 35 (2012) 102–107.
[2] I. Földvari, A. Baraldi, R. Capelletti, N. Magnani, R.F. Sosa, A.F. Munoz, L.A. Kappers, A. Watterich, Opt. Mater. 29 (2007) 688–696.
[3] Yanmin Yang, Baoquan Yao, Baojiu Chen, Cheng Wang, Guozhong Ren, Xiaojun Wang, Opt. Mater. 29 (2007) 1159–1165.
[4] Y.K. Voronko, A.A. Kaminsky, V.L. Osiko, A.M. Prokhorov, Sov. Phys. – JETP Lett. 1 (1965) 3–5.
[5] L.F. Johnson, J. Appl. Phys. Lett. 19 (1971) 44–47.
[6] Bo Zhou, Yue-Bun Pun Edwin, Hai Lin, Yang Dianlai, Lihui Huang, J. Appl. Phys. 106 (2009) 103105.
[7] G. Dominiak-Dzik, S. Golab, J. Zawadzka, W. Ryba-Romanowski, T. lukasiewicz, M. Swirkowicz, J. Phys.: Condens. Matter 10 (1998) 10291–10306.
[8] Li Feng, Jing Wang, Qiang Tang, Lifang Liang, Hongbin Liang, Su Qiang, J. Lumin. 124 (2007) 187–194.
[9] E.V. Koporulina, N.I. Leonyuk, D. Hansen, K.L. Bray, J. Cryst. Growth 191 (1998) 767–773.
[10] K.-C. Liang, R.P. Chaudhury, B. Lorenz, Y.Y. Sun, L.N. Bezmaternykh, V.L. Temerov, C.W. Chu, Phys. Rev. B 83 (2011) 180417.
[11] A. Baraldi, R. Capelletti, M. Mazzera, N. Magnani, I. Földvári, E. Beregi, Phys. Rev. B 76 (2007) 165130.
[12] J. Li, J. Wang, H. Tan, X. Cheng, F. Song, H. Zhang, S. Zhao, J. Cryst. Growth 256 (2003) 324–327.
[13] V.L. Temerov, A.E. Sokolov, A.L. Sukhachev, A.F. Bovina, I.S. Edelman, A.V. Malakhovskii, Crystallogr. Rep. 53 (2008) 1157.
[14] A.V. Malakhovskii, T.V. Kutsak, A.L. Sukhachev, A.S. Aleksandrovsky, A.S. Krylov, I.A. Gudim, M.S. Molokeev, Chem. Phys. 428 (2014) 137–143.
[15] B.R. Judd, Phys. Rev. 127 (1962) 750.
[16] G.S. Ofelt, Chem. Phys. 37 (1962) 511.
[17] A.V. Malakhovskiĭ, A.É. Sokolov, V.L. Temerov, L.N. Bezmaternykh, A.L. Sukhachev, V.A. Seredkin, S.L. Gnatchenko, I.S. Kachur, V.G. Piryatinskaya, Phys. Solid State 50 (2008) 1287–1293.
[18] A.A. Kaminskii, Crystalline Lasers: Physical processes and Operating Schemes, CRC Press, New York, London, Tokyo, 1996.
[19] B.M. Walsh, G.W. Grew, N.P. Barnes, J. Phys. Chem. Solids 67 (2006) 1567–1582.
[20] Q. Su, Q.Y. Wang, S.X. Wu, Chin. J. Lasers 16 (1989) 612.
[21] N. Rakov, G.S. Maciel, C.B. de Araujo, J. Appl. Phys. 91 (2002) 1272.
[22] X. Wang, H. Lin, D. Yang, L. Lin, E.Y.B. Pun, J. Appl. Phys. 101 (2007) 113535.
[23] M.R. Reddy, S.B. Raju, N. Veeraiah, J. Phys. Chem. Solids 61 (2000) 1567.
[24] W.F. Krupke, Phys. Rev. 145 (1966) 325.
[25] J.A. Caird, L.G. DeShazer, IEEE J. Quant. Electron. QE-11 (1975) 97–99.
[26] D. Kasprowicz, M.G. Brik, A. Majchowski, E. Michalski, A. Biadasz, J. Alloys Compd. 509 (2011) 1430–1435.
[27] A.S. Aleksandrovsky, A.V. Malakhovskii, A.S. Krylov, V.N. Voronov, J. Lumin. 132 (2012) 690.
[28] N.V. Karlov, Lectures on Quantum Electronics, CRC Press, 1992.
[29] P. Goldner, Mol. Phys. 101 (2003) 903.
[30] W.F. Krupke, IEEE J. Quant. Electron. QE-10 (1974) 450.